SOIL Discuss., 1, 401–428, 2014
www.soil-discuss.net/1/401/2014/
doi:10.5194/soild-1-401-2014

Depth distribution of radiocesium in Fukushima paddy fields and implications for ongoing decontamination works

H. Lepage[1], O. Evrard[1], Y. Onda[2], I. Lefèvre[1], J. P. Laceby[1], and S. Ayrault[1]

[1]Laboratoire des Sciences du Climat et de l'Environnement (LSCE), Unité Mixte de Recherche 8212 (CEA-CNRS-UVSQ/IPSL), Gif-sur-Yvette, France
[2]Graduate School of Life and Environmental Sciences, Center for Research in Isotopes and Environmental Dynamics (CRIED), University of Tsukuba, Tsukuba, Japan

Received: 9 September 2014 – Accepted: 11 September 2014 – Published: 19 September 2014

Correspondence to: H. Lepage (hugo.lepage@lsce.ipsl.fr)

Published by Copernicus Publications on behalf of the European Geosciences Union.

Abstract

Large quantities of radiocesium were deposited across a $3000\,km^2$ area northwest of the Fukushima Dai-ichi nuclear power plant after the March 2011 accident. Although many studies have investigated the fate of radiocesium in soil in the months following the accident, the potential migration of this radioactive contaminant in rice paddy fields requires further examination after the typhoons that occurred in this region. Such investigations will help minimize potential human exposure in rice paddy fields or transfer of radioactive contaminants from soils to rice. Radionuclide activity concentrations and organic content were analysed in 10 soil cores sampled from paddy fields in November 2013, 20 km north of the Fukushima power plant. Our results demonstrate limited depth migration of radiocesium with the majority concentrated in the uppermost layers of soils (< 5 cm). More than 30 months after the accident, 81.5 to 99.7 % of the total ^{137}Cs inventories was still found within the < 5 cm of the soil surface, despite cumulative rainfall totalling 3300 mm. Furthermore, there were no significant correlations between radiocesium migration depth and total organic carbon content. We attributed the maximum depth penetration of ^{137}Cs to maintenance (grass cutting – 97 % of ^{137}Cs in the upper 5 cm) and farming operations (tilling – 83 % of ^{137}Cs in the upper 5 cm). As this area is exposed to erosive events, ongoing decontamination works may increase soil erodibility. We therefore recommend the rapid removal of the uppermost – contaminated – layer of the soil after removing the vegetation to avoid erosion of contaminated material during the subsequent rainfall events. Remediation efforts should be concentrated on soils characterised by radiocesium activities > 10 000 $Bq\,kg^{-1}$ to prevent the contamination of rice. Further analysis is required to clarify the redistribution of radiocesium eroded on river channels.

SOILD
1, 401–428, 2014

1 Introduction

The Tohoku earthquake and the subsequent tsunami on 11 March 2011 resulted in the Fukushima Dai-Ichi Nuclear Power Plant (FDNPP) accident and the significant corresponding atmospheric release of radionuclides, such as ^{137}Cs ($T_{1/2}$ = 30 years) (Saunier et al., 2013). Approximately 80% of the release was transported over the Pacific Ocean with the remainder predominantly deposited on Fukushima Prefecture soils as a result of wet atmospheric fallout (Kawamura et al., 2011). Estimations of ^{137}Cs total activity in the Fukushima Prefecture soils range between 10 PBq and 760 PBq, with deposition characterised by strong spatial heterogeneities (Koo et al., 2014). The highest activities are concentrated within a 70 km long radioactive plume where initial ^{137}Cs contamination exceeded 300 kBq m^{-2} covering an area of 3000 km^2. Therefore it is crucial to understand and monitor the fate of the initial radioactive deposits in order to protect the local population against exposure to high dose rates that may prevail in areas accumulating contamination.

In the coastal catchments affected by the FDNPP accident, Chartin et al. (2013) showed that paddy fields are one of the major sources of ^{137}Cs mobilization and export by soil erosion. A significant proportion of paddy fields are located in the upstream area of the contaminated catchments and they were shown to supply large quantities of contaminated sediment to rivers during typhoons and snowmelt events (Evrard et al., 2013; Evrard et al., 2014). Dispersion of contamination originating from paddy fields along the rivers of the region could therefore contaminate downstream areas that were relatively low affected by the initial fallout.

Several studies have shown that radiocesium has a low mobility in most soils and is rapidly fixed to fine particles, especially clay minerals (Sawhiney, 1972; He and Walling, 1996). These findings were confirmed in the vicinity of the main contamination plume in the Fukushima Prefecture where Saito et al. (2014) reported that ^{137}Cs was concentrated in the silt and clay fractions. Also, it was reported that the majority of ^{137}Cs remained in the first centimetre of the soil profile (Fujiwara et al., 2012; Kato et al.,

SOILD
1, 401–428, 2014

2012; Koarashi et al., 2012; Lepage et al., 2014). However, it was also shown that in soils with high content of organic matters, radiocesium may migrate down the soil profile as organic matter may reduce its affinity with clay minerals (Kamei-Ishikawa et al., 2008; Koarashi et al., 2012; Staunton et al., 2002; Szenknect et al., 2003).

The main soil type found in paddy fields located in the main contamination plume is Andosol (Endo et al., 2013; Nakao et al., 2014; Takeda et al., 2014), characterized by high contents of organic matter (Kamei-Ishikawa et al., 2008; Takeda et al., 2004). The potential migration of radiocesium with depth should be specifically investigated in these soils. Takeda et al. (2014) showed a low adsorption of radiocesium in a soybean field composed of Andosols. This low Radiocesium Interception Potential (RIP) could be due to the high amount of amorphous minerals in these soils (Vandebroek et al., 2012). Investigating the specific migration of radiocesium with depth in a selection of Andosols located within the main contamination plume of Fukushima Prefecture is therefore crucial, as the transfer factor from the soil to the crops is higher in substrates characterised by low RIP values (Takeda et al., 2014). This investigation of radiocesium migration in paddy fields is particularly timely in the current post-accidental phase characterised by the implementation of large-scale remediation efforts targeting paddy fields. The implications of these findings for contamination transfer to crops and potential soil erosion will be specifically discussed.

2 Materials and methods

2.1 Study area

The study was conducted in Fukushima Prefecture, located in North-Eastern Japan, 30 km northwest of FDNPP (Fig. 1). We focused our work on two coastal catchments (i.e. Mano and Nitta River catchments; 450 km^2) draining the main part of the radioactive plume. These catchments extend from the coastal mountain range (approximately 30 km from the coast) to the Pacific Ocean, and their elevation ranges from

0 to 900 m. Mean annual rainfall was 1320 mm according to Japanese Meteorological Agency (2014) measured over 37 years at the rainfall station located in the upper part of the Nitta catchment (Fig. 1). Our study was conducted in November 2013 and cumulative rainfall reached 3300 mm (max = 35 mm h^{-1}) between the accident and our field survey (32 months) with the occurrence of 4 typhoons (Songda and Roke in 2011, Man-Yi and Wipha in 2013). In these catchments, paddy fields are predominantly located along the rivers with irrigation generally performed from May to September (Tanaka et al., 2013).

Remediation works implemented since July 2012 under the supervision of the Japanese Ministry Of Environment (MOE, 2012a, 2013) are concentrated in upper parts of the Nitta River catchment and consist of removing the five uppermost centimetres of the soil (Mizoguchi, 2013; Sakai et al., 2014) to decrease the radioactive dose level in order to avoid exceeding the permissible level (1 mSv yr^{-1}) determined by Japanese authorities (MOE, 2012b).

2.2 Sample collection and preparation

A radiameter (LB123 D-H10, Berthold Technologies) was used to measure radiation dose rates at the ground level in the paddy fields (Table 1). To be representative, dose levels were measured at 5 different locations on each field. The formula Eq. (1) proposed by the Ministry of Environment MOE (2012b) was then applied to convert these data into annual dose rates.

$$D_{an} = \frac{(D_{amb} - 0.04) \cdot (8 + 16 \cdot 0.4) \cdot 365}{1000}, \quad (1)$$

where D_{amb} is the ambient dose rate, and D_{an} is the annual dose rates.

Soil cores (Table 1) were collected in paddy fields across the two selected catchments (Fig. 1). We selected the fields depending on their dose rate to investigated migration of radiocesium in field with different levels of contamination (Table 1).

SOILD
1, 401–428, 2014

A soil auger (diameter 45 mm) was used to sample soil cores to a depth of 10 cm from 10 fields. The soil cores were sub-sectioned into 1 cm increment layers for the uppermost 5 cm, and into a 5 cm interval to a depth of 10 cm. Because of the very high radioactive dose rate measured at the location where core P9 was sampled (5.5 µsv h^{-1}), two additional layers were sampled at greater depths (10–15 and 15–20 cm). Mean compaction in the cores was estimated to 13 % using density of the soil.

2.3 Gamma spectrometry measurements

Before measurement, samples were dried in an oven at 40 °C for a week, ground to a fine powder in an agate mortar, and then packed into 15 mL polyethylene specimen container. Cesium-137 activities were determined by gamma spectrometry using low-background coaxial N- and P-types HPGe detectors (Canberra/Ortec). Counting times of samples varied between 80 000 s and 150 000 s. The ^{137}Cs activities were measured at the 661 keV emission peak. Counting efficiencies and energy calibration were monitored using internal and certified International Atomic Energy Agency (IAEA) reference materials prepared in the same specimen containers as the samples. Uncertainties on results were estimated by combining counting statistics and calibration uncertainties. Summing and self-absorption effects were taken into account by measuring reference materials with similar densities and characteristics as the collected samples. All activities were decay corrected to the date of 14 March 2011 corresponding to the date of the main radionuclide deposits on soils (Kinoshita et al., 2011; Shozugawa et al., 2012).

2.4 Total Organic Carbon (TOC) measurements

The dried and ground samples were analysed in a total organic carbon analyser (VarioTOC, Elementar) following the High Temperature and Catalytic Oxidation (HTCO) method. The catalytic oxidation extracts the total carbon of the sample as carbon dioxide in an oven (950 °C) with the use of copper oxide as catalyser. The CO_2 produced

SOILD
1, 401–428, 2014

was then analysed by an infrared detector. To determine the organic fraction of the Carbon (TOC), 300 µL of hydrochloric acid was added to remove inorganic carbon and the samples were dried at 105 °C. The analysis was then repeated. Data reproducibility was examined by replicate analyses of selected samples and uncertainties were determined using Organic Analytical Standard (Elemental microanalysis, Okehampton).

2.5 Migration of ^{137}Cs with depth

Radiocesium profiles in undisturbed soils are expected to display an exponential decline with depth (He and Walling, 1997; Walling and He, 1999), which can be described by the following function (Beck, 1966):

$$C_{(x)} = C_0(1 - \exp^{-\alpha.x}), \tag{2}$$

where $C_{(x)}$ is the concentration activity of a radionuclide in Bq kg^{-1} at the depth x (cm) and C_0 at $x = 0$, and α (cm^{-1}) is a coefficient representing the characteristics of the radionuclide distribution and depends on different characteristics of the soil (pH, CEC, TOC, clay content).

In addition, a more specific model can be used to describe ^{137}Cs mobility in soils (Kato et al., 2012; Koarashi et al., 2012; Miller et al., 1990):

$$I_{(x)} = I_t(1 - \exp^{-x/h0}), \tag{3}$$

where $I_{(x)}$ is the radiocesium inventory (Bq m^{-2}) at the x (kg m^{-2}) depth, I_t is the total ^{137}Cs inventory and h_0 is the relaxation mass depth (kg m^2), an index characterising the radiocesium penetration in the soil. The greater the value of the relaxation mass depth h_0, the deeper the ^{137}Cs penetrates into the soil profile.

2.6 Rice transfer factor

Endo et al. (2013) investigated the contamination of rice in the vicinity of the FDNPP and estimated the transfer factor (TF) from Andosols to polished rice to be 0.01.

SOILD
1, 401–428, 2014

The estimation of contaminated polished rice harvested on paddy field could be determined using Eq. (4):

$$A_{pr} = \mathrm{TF} \cdot A_s, \tag{4}$$

where A_{pr} (Bq kg^{-1}) is the radiocesium activity in polished rice, A_s (Bq kg^{-1}) is the average radiocesium activity in associated dried soil from the surface to a depth of 15 cm and TF the transfer factor from soil to polished rice.

3 Results and discussion

3.1 Migration with depth

Based on the evolution of radiocesium activity with depth, soil cores were classified into four groups (uncontaminated, tilled, managed and undisturbed) (Table 2) (Figs. 2 and 4).

Uncontaminated core P5 (Fig. 2) did not show evidence of additional contamination due to Fukushima accident. At this site the ^{137}Cs concentration levels remained similar to pre-accident conditions, which were estimated not to exceed 100 Bq kg^{-1} in Japanese soils (Fukuyama et al., 2005). The similar level of contamination observed along the entire P5 core (Fig. 2) is likely due to tilling by heavy farming machinery (Endo et al., 2013; Matsunaga et al., 2013; Yamaguchi et al., 2012) (Fig. 3a). According to Fig. 1, this field was contaminated following the dispersion of contamination, but it has been decontaminated as the actual core display the absence of Fukushima derived contamination. This paddy field is now available to rice culture.

P2 and P4 were fully disturbed after the initial radionuclide deposition resulting in a homogenization of activities in successive soil layers (Fig. 4). These fields were most likely tilled by farmers and now around 17 % of the total contamination inventory is found in the deeper layers (i.e. 5–10 cm) (Table 2) This percentage could be higher (≈ 30 %) as tilled soil generally show a similar level of contamination until 15 cm (Endo et al., 2013; Yamaguchi et al., 2012). The ongoing farming operations in this area can be explained by the fact that fields are not located in the evacuation-prepared area and that cultivation is allowed (Fig. 1).

Managed fields differ from tilled fields as only the upper 3 centimetres show a similar level of contamination (Fig. 4) and less than 10 % of the contamination is beneath 5 cm. In undisturbed fields, our results demonstrated that more than 90 % of the radiocesium contamination was concentrated in the 5 upper centimetres (Table 2). These results confirm those found for undisturbed soils located under different land uses in the vicinity of the FDNPP (Fig. 5) by previous studies (Table 3). Most of them concluded that radiocesium was exclusively found in the 5 uppermost centimetres of the undisturbed soil (92–100 %). Our results on tilled soils are also consistent with those from previous publications (50–83 %).

TOC analyses (Table 2) confirmed that most fields sampled in upper parts of the catchments (P3, P7, P8, P9 and P10 sites; Fig. 1) are likely constituted of Andosols because of their higher level of TOC (2.1–8.5 %) than the one measured in fields of the coastal plains (1.0–1.6 %). Overall, despite this difference in TOC content observed between the soil cores, no significant correlation was found between TOC and both the α coefficient ($r = -0.35$, $p(95\,\%) = 0.44$) and the relaxation mass depth (h_0; $r = -0.30$, $p(95\,\%) = 0.51$). As the migration depth of radiocesium in soils does not vary with the soil type, the difference between both soil groups is most likely explained by the type and frequency of farming operations carried out between the nuclear accident and the sampling campaign.

A group of undisturbed fields (P6, P7 and P9) remained abandoned by the end of 2013, as they show an exponential decrease of radiocesium activities with depth following Eq. (2) (Fig. 4). During our sampling campaign, P9 was still undisturbed (Fig. 3c) as it was protected by a dense grass cover. P6 and P7 showed evidence of recent farming operations but the dense grass cover indicates that mowing is conducted with a low frequency (Fig. 3b). Furthermore, our results on relaxation mass depths (h_0) in undisturbed soils (Table 2) varied from 5.4 to 8.3 and remained in the same range as

SOILD
1, 401–428, 2014

previous results found for soils collected in this area (Fujiwara et al., 2012; Kato et al., 2012; Koarashi et al., 2012; Lepage et al., 2014; Matsunaga et al., 2013) (Table 3). Even if this result indicates a low migration of radiocesium, contamination from the FD-NPP accident could still be found at the 10–15 and 15–20 cm layers in P9 (respectively 370 and 170 Bq kg^{-1}, see Fig. 2).

In contrast, managed fields (P1, P3, P8 and P10) show a similar level of contamination in the upper three centimetres and then a decrease (Fig. 4). P8 differs from the other cores of the group as a similar level of contamination is only observed in the uppermost 2 cm of the soil. These fields have been continuously managed since the accident, as illustrated by our field observations during previous campaigns (November 2011, April 2012 and May 2013). Grass was cut each year using heavy machinery, which may explain the mixing of soil and associated radiocesium in these fields due to the compaction of the first centimetres of the soil (Jagercikova et al., 2014; Matsunaga et al., 2013). Takahashi et al. (2014) also reported the same migration in the uppermost 3 cm (Table 3) and concluded that it was caused by the repeated formation and melting of needle ice in the surface soil during winter. Investigation should be done to clarify the process involved in this migration.

To complement the published research conducted a few months after the accident (Fig. 6), our results show that even more than 30 months after the accident and after the occurrence of several typhoons (Fig. 6) the in-depth migration of radiocesium is very low with the majority (93–99 %) of this radionuclide still found in the upper 5 cm of undisturbed and managed soils. Those results are complementary with the study of Mastunaga et al. (2013) who concluded that radiocesium did not migrate with depth even after rainfalls, 5 months after the accident. Tilling is the main contributor of the migration of radiocesium in soil as there is an important part of contamination under the first layers (50–83 %) in tilled field (Table 3).

SOILD
1, 401–428, 2014

3.2 Transfer of contamination to the rice

Based on the research of Endo et al. (2013), we estimated the quantity of radiocesium that could be found in polished rice harvested on all the studied fields using Eq. (4) (Table 4). As an estimate of the contamination from 10 to 15 cm is required for this formula, we defined the contamination level to be the same as the above layer (5–10 cm) for undisturbed and managed soil (≈ 1 % of the total contamination). This will maximise the estimation of contamination in the rice. As a similar level of contamination is generally observed in the first 15 cm for tilled soil, we attributed to the 10–15 cm layer the average contamination level of the upper layers.

Based on the current level of contamination, 3 fields displayed an excessive level of contamination for the cultivation of rice (P7, P9 and P10) (Table 4). Decontamination by removing the upper 5 cm will allow them to contain less than 10 000 Bq kg^{-1} in each layer and meeting contamination levels under the permissible level.

According to Eq. (2) and using $\alpha = 1.2\,cm^{-1}$ (the mean of the undisturbed fields), the permissible level in rice could be reached in undisturbed or managed field where initial deposition was higher than 150 kBq kg^{-1}. This contamination level increases to 60 000 kBq kg^{-1} in the case of remediation effort with the assumption that the upper 5 cm were removed. In decontaminated but tilled fields, only 225 kBq kg^{-1} as deposited contamination is needed to reach the permissible level. To avoid this type of potential rice contamination, we highly recommend not tilling any field with ambient dose level exceeding the permissible level of 1 msv yr^{-1}. In fields already tilled, we recommend to remove at least 15 cm.

3.3 Erosion transfer of contaminants

In most of the investigated soil cores, contamination is concentrated in the upper layers of the soils and is therefore potentially available for soil erosion (Motha and Wallbrink, 2002; Walling and Woodward, 1992). However, in abandoned fields, the dense grass cover will protect the soil against erosion as soil erodibility is mainly controlled by the

SOILD
1, 401–428, 2014

vegetation cover, surface roughness and crusting characteristics (Evrard et al., 2008; Le Bissonnais et al., 2005). During decontamination operations, the grass is cut and vegetation is removed leaving the soil bare and exposed to the erosive impact of intense rainfall. The specific supply of contaminated sediment from fields where remediation efforts were concentrated to nearby rivers was demonstrated by Evrard et al. (2014) who showed an increase of radioactive dose rates in recent sediment drape deposits collected in upper parts of the Nitta River catchment after the heavy typhoons that occurred during summer in 2013.

In this context, we recommend to rapidly remove the first centimetres of the soil immediately after removing the vegetation to avoid erosion of contaminated material during the subsequent rainfall events. Alternatively, remediation efforts could be concentrated before July or after October, when typhoons are unlikely to occur. We do not recommend mixing soil with water (puddling) in contaminated fields, as this could export the contamination contained in the uppermost layers of the soil (Wakahara et al., 2013). Furthermore, decontaminated fields could be re-contaminated by the supply of contaminated particles stored in other places such as grasslands, forests or river channel (Sakai et al., 2014). To avoid this recontamination, we recommend to start the decontamination works in upper catchment parts and to proceed seaward.

4 Concluding remarks

We collected soil surface cores in paddy fields during a sampling campaign in November 2013 to investigate the migration of radiocesium in soils contaminated after the FDNPP accident (March 2011). We attributed the maximum depth penetration of ^{137}Cs to maintenance and farming operations in the fields as tilled field showed a similar level of contamination in each layer while in managed field, where vegetation was removed, contamination only migrated down the first 3 cm. In undisturbed soils, radiocesium inventory decreased with depth following an exponential function. Our results confirm the overall low migration of radiocesium concentrated in the first centimetres (< 5 cm) of

SOILD
1, 401–428, 2014

Andosols in undisturbed and managed paddy fields located within the main Fukushima contamination plume.

As decontamination works may increase soil sensitivity to erosion, we recommend to remove the uppermost – contaminated – layer of the soil as soon as possible after the removal of vegetation. This decontamination work should be done before July or after October, when typhoons are unlikely to occur.

Remediation efforts should be concentrated on soils characterised by radiocesium activities > 10 000 Bq kg^{-1} to prevent contamination of the rice that will be re-cultivated in future in this region. Fields with ambient dose levels higher than the permissible level should not be tilled or removing only the upper 5 cm will not be sufficient and could result in the contamination of rice in the future.

The Supplement related to this article is available online at doi:10.5194/soild-1-401-2014-supplement.

Author contributions. H. Lepage and O. Evrard wrote the main manuscript; O. Evrard and Y. Onda designed research; H. Lepage and O. Evrard conducted field sampling; H. Lepage and I. Lefèvre conducted laboratory measurements. Y. Onda, J. P. Laceby and S. Ayrault participated to the redaction and reviewed the manuscript.

Acknowledgements. This work has been supported by ANR (*French National Research Agency*) and JST (*Japan Science and Technology agency*) in the framework of the joint TOFU ANR Flash/J-RAPID Franco-Japanese project (ANR-11-JAPN-001). This work has also been supported by CNRS in the framework of the NEEDS-Environnement HAMUSUTA project, and by the Institute of Environmental Radioactivity (IER) in Fukushima University. Finally, funding from ANR in the framework of the AMORAD project (ANR-11-RSNR-0002) is gratefully acknowledged. Hugo Lepage received a PhD fellowship from CEA (Commissariat à l'Energie Atomique et aux Energies Alternatives, France). The authors are also very grateful to Aurélie Ritt for conducting TOC measurements.

References

Beck, H. L.: Environmental gamma radiation from deposited fission products, Health Phys., 12, 313–322, 1966.

Chartin, C., Evrard, O., Onda, Y., Patin, J., Lefèvre, I., Ottlé, C., Ayrault, S., Lepage, H., and Bonté, P.: Tracking the early dispersion of contaminated sediment along rivers draining the Fukushima radioactive pollution plume, Anthropocene, 1, 23–34, 2013.

Columbus, C.: How I Discovered America, Hispanic Press, Barcelona, 1492.

Endo, S., Kajimoto, T., and Shizuma, K.: Paddy-field contamination with 134Cs and 137Cs due to Fukushima Dai-ichi Nuclear Power Plant accident and soil-to-rice transfer coefficients, J. Environ. Radioactiv., 116, 59–64, 2013.

Evrard, O., Vandaele, K., Bielders, C., and Van Wesemael, B.: Seasonal evolution of runoff generation on agricultural land in the Belgian loess belt and implications for muddy flood triggering, Earth Surf. Proc. Land, 1301, 1285–1301, 2008.

Evrard, O., Chartin, C., Onda, Y., Patin, J., Lepage, H., Lefèvre, I., Ayrault, S., Ottlé, C., and Bonté, P.: Evolution of radioactive dose rates in fresh sediment deposits along coastal rivers draining Fukushima contamination plume, Sci. Rep. 3, 3079, doi:10.1038/srep03079, 2013.

Evrard, O., Chartin, C., Onda, Y., Lepage, H., Cerdan, O., Lefèvre, I., and Ayrault, S.: Renewed soil erosion and remobilisation of radioactive sediment in Fukushima coastal rivers after the 2013 typhoons, Sci. Rep., 4, 4574, doi:10.1038/srep04574, 2014.

Fujiwara, T., Saito, T., and Muroya, Y.: Isotopic ratio and vertical distribution of radionuclides in soil affected by the accident of Fukushima Dai-ichi nuclear power plants, J. Environ. Radioactiv., 113, 37–44, 2012.

Fukuyama, T., Takenaka, C., and Onda, Y.: 137Cs loss via soil erosion from a mountainous headwater catchment in central Japan, Sci. Total Environ., 350, 238–247, 2005.

He, Q. and Walling, D.: Interpreting particle size effects in the adsorption of 137Cs and unsupported 210Pb by mineral soils and sediments, J. Environ. Radioactiv., 30, 117–137, 1996.

He, Q. and Walling, D.: The distribution of fallout 137Cs and 210Pb in undisturbed and cultivated soils, Appl. Radiat. Isotopes, 48, 677–690, 1997.

Jagercikova, M., Evrard, O., Balesdent, J., Lefèvre, I., and Cornu, S.: Modeling the migration of fallout radionuclides to quantify the contemporary transfer of fine particles in Luvisol profiles under different land uses and farming practices, Soil Till. Res., 140, 82–97, 2014.

SOILD

1, 401–428, 2014

Depth distribution of radiocesium in Fukushima paddy fields

H. Lepage et al.

Japanese Meteorological Agency: available at: http://www.data.jma.go.jp/obd/stats/etrn/view/annually_a.php?prec_no=36&block_no=1150&year=2013&month=4&day=&view=, last access: 28 July 2014 (in Japanese).

Kamei-Ishikawa, N., Uchida, S., and Tagami, K.: Distribution coefficients for 85Sr and 137Cs in Japanese agricultural soils and their correlations with soil properties, J. Radioanal. Nucl. Ch., 277, 433–439, 2008.

Kato, H., Onda, Y., and Teramage, M.: Depth distribution of 137Cs, 134Cs, and 131I in soil profile after Fukushima Dai-ichi Nuclear Power Plant Accident, J. Environ. Radioactiv., 111, 59–64, 2012.

Kawamura, H., Kobayashi, T., Furuno, A., In, T., Ishikawa, Y., Nakayama, T., Shima, S., and Awaji, T.: Preliminary numerical experiments on oceanic dispersion of 131I and 137Cs discharged into the ocean because of the Fukushima Daiichi nuclear power plant, J. Nucl. Sci. Technol., 48, 1349–1356, 2011.

Kinoshita, N., Sueki, K., Sasa, K., Kitagawa, J., Ikarashi, S., Nishimura, T., Wong, Y.-S., Satou, Y., Handa, K., Takahashi, T., Sato, M., and Yamagata, T.: Assessment of individual radionuclide distributions from the Fukushima nuclear accident covering central-east Japan, P. Natl. Acad. Sci. USA, 108, 19526–19529, 2011.

Koarashi, J., Atarashi-Andoh, M., Matsunaga, T., Sato, T., Nagao, S., and Nagai, H.: Factors affecting vertical distribution of Fukushima accident-derived radiocesium in soil under different land-use conditions, Sci. Total Environ., 431, 392–401, 2012.

Koo, Y.-H., Yang, Y.-S., and Song, K.-W.: Radioactivity release from the Fukushima accident and its consequences: A review, Prog. Nucl. Energ., 74, 61–70, 2014.

Le Bissonnais, Y., Cerdan, O., Lecomte, V., Benkhadra, H., Souchère, V., and Martin, P.: Variability of soil surface characteristics influencing runoff and interrill erosion, Catena, 62, 111–124, 2005.

Lepage, H., Evrard, O., Onda, Y., Patin, J., Chartin, C., Lefèvre, I., Bonté, P., and Ayrault, S.: Environmental mobility of 110 mAg: lessons learnt from Fukushima accident (Japan) and potential use for tracking the dispersion of contamination within coastal catchments, J. Environ. Radioactiv., 130, 44–55, 2014.

Matsunaga, T., Koarashi, J., Atarashi-Andoh, M., Nagao, S., Sato, T., and Nagai, H.: Comparison of the vertical distributions of Fukushima nuclear accident radiocesium in soil before and after the first rainy season, with physicochemical and mineralogical interpretations, Sci. Total Environ., 447, 301–314, 2013.

SOILD

1, 401–428, 2014

METI: Areas to which evacuation orders have been issued (April 1, 2014), available at: http://www.meti.go.jp/english/earthquake/nuclear/roadmap/pdf/140401MapOfAreas.pdf (last access: 26 August 2014), 2014.
MEXT: MEXT, Japan, available at: http://radioactivity.nsr.go.jp/ja/contents/7000/6289/24/203_0928.pdf (last access: 26 August 2014), 2012 (in Japanese).
MHLW: New standard limits for radionuclides in foods, available at: http://www.mhlw.go.jp/english/topics/2011eq/dl/new_standard.pdf (last access: 26 August 2014), 2011.
Miller, K. M., Kuiper, J. L., and Heifer, I. K.: 137Cs Fallout Depth Distributions in Forest Versus Field Sites: Implications for External Gamma Dose Rates, J. Environ. Radioactiv., 12, 23–47, 1990.
Mizoguchi, M.: Remediation of Paddy Soil Contaminated by Radiocesium in Iitate Village in Fukushima Prefecture, Agric. Implic. Fukushima Nucl., 131–142, 2013.
MOE: available at: http://josen.env.go.jp/en/ (last access: 26 August 2014), 2012a.
MOE: available at: http://josen.env.go.jp/osen/osen_05.html (last access: 26 August 2014), 2012b (in Japanese).
MOE: Progress on Off-site Cleanup efforts in Japan, available at: http://josen.env.go.jp/en/documents/pdf/workshop_july_17-18_2013_01.pdf (last access: 26 August 2014), 2013.
Motha, J. and Wallbrink, P.: Tracer properties of eroded sediment and source material, Hydrol. Process., 16, 1983–2000, 2002.
Nakao, A., Ogasawara, S., Sano, O., Ito, T., and Yanai, J.: Radiocesium sorption in relation to clay mineralogy of paddy soils in Fukushima, Japan, Sci. Total Environ., 468–469, 523–529, 2014.
Saito, T., Makino, H., and Tanaka, S.: Geochemical and grain-size distribution of radioactive and stable cesium in Fukushima soils: implications for their long-term behavior, J. Environ. Radioactiv., 138C, 11–18, 2014.
Sakai, M., Gomi, T., Nunokawa, M., Wakahara, T., and Onda, Y.: Soil removal as a decontamination practice and radiocesium accumulation in tadpoles in rice paddies at Fukushima, Environ. Pollut., 187, 112–115, 2014.
Saunier, O., Mathieu, A., Didier, D., Tombette, M., Quélo, D., Winiarek, V., and Bocquet, M.: An inverse modeling method to assess the source term of the Fukushima Nuclear Power Plant accident using gamma dose rate observations, Atmos. Chem. Phys., 13, 11403–11421, doi:10.5194/acp-13-11403-2013, 2013.

SOILD
1, 401–428, 2014

Depth distribution of radiocesium in Fukushima paddy fields

H. Lepage et al.

Sawhiney, B.: Selective sorption and fixation of cations by clay minerals: a review, Clay. Clay Miner., 20, 93–100, 1972.
Shozugawa, K., Nogawa, N., and Matsuo, M.: Deposition of fission and activation products after the Fukushima Dai-ichi nuclear power plant accident, Environ. Pollut., 163, 243–247, 2012.
Staunton, S., Dumat, C., and Zsolnay, A.: Possible role of organic matter in radiocaesium adsorption in soils, J. Environ. Radioactiv., 58, 163–73, 2002.
Szenknect, S., Gaudet, J. P., and Dewiere, L.: Evaluation of distribution coefficients for the prediction of strontium and cesium migration in a natural sand at different water contents, J. Phys. IV, 107, 1279–1282, 2003.
Takahashi, J., Tamura, K., and Suda, T.: Vertical distribution and temporal changes of 137Cs in soil profiles under various land uses after the Fukushima Dai-ichi Nuclear Power Plant accident, J. Environ. Radioactiv., in press, 2014.
Takeda, A., Kimura, K., and Yamasaki, S.: Analysis of 57 elements in Japanese soils, with special reference to soil group and agricultural use, Geoderma, 119, 291–307, 2004.
Takeda, A., Tsukada, H., Yamaguchi, N., Takeuchi, M., Sato, M., Nakao, A., and Hisamatsu, S.: Relationship between the radiocesium interception potential and the transfer of radiocesium from soil to soybean cultivated in 2011 in Fukushima Prefecture, Japan, J. Environ. Radioactiv., 137, 119–124, 2014.
Tanaka, K., Takahashi, Y., and Sakaguchi, A.: Vertical profiles of iodine-131 and cesium-137 in soils in Fukushima prefecture related to the Fukushima Daiichi Nuclear Power Station accident, Geochem. J., 46, 73–76, 2012.
Tanaka, K., Iwatani, H., Takahashi, Y., Sakaguchi, A., Yoshimura, K., and Onda, Y.: Investigation of spatial distribution of radiocesium in a paddy field as a potential sink, PLoS One, 8, e80794, doi:10.1371/journal.pone.0080794, 2013.
Teramage, M. T., Onda, Y., Patin, J., Kato, H., Gomi, T., and Nam, S.: Vertical distribution of radiocesium in coniferous forest soil after the Fukushima nuclear power plant accident, J. Environ. Radioactiv., 137, 37–45, 2014.
Vandebroek, L., Van Hees, M., Delvaux, B., Spaargaren, O., and Thiry, Y.: Relevance of Radiocaesium Interception Potential (RIP) on a worldwide scale to assess soil vulnerability to 137Cs contamination, J. Environ. Radioactiv., 104, 87–93, 2012.
Wakahara, T., Onda, Y., and Kato, H.: Estimation of radionuclide discharge from paddy fields in two experimental plots with different initial scrapings after the Fukushima Dai-ichi Nuclear Power Plant accident 1–3, 2013.

SOILD
1, 401–428, 2014

Walling, D. E. and He, Q.: Improved models for estimating soil erosion rates from cesium-137 measurements, J. Environ. Qual., 28, 611–622, 1999.
Walling, D. E. and Woodward, J. C.: Use of radiometric fingerprints to derive information on suspended sediment sources, Eros. Sediment Transp. Monit. Program. River Basin, 210, 153–164, 1992.
Yamaguchi, N., Eguchi, S., Fujiwara, H., Hayashi, K., and Tsukada, H.: Radiocesium and radioiodine in soil particles agitated by agricultural practices: field observation after the Fukushima nuclear accident, Sci. Total Environ., 425, 128–134, 2012.

SOILD
1, 401–428, 2014

Depth distribution of radiocesium in Fukushima paddy fields

H. Lepage et al.

Table 1. Location of investigated soil cores and ambient radioactive dose rates measured at the ground level. Annual dose rates exceeding the permissible level of 1 $mSv\,yr^{-1}$ are indicated in bold (MOE, 2012b).

Latitude	Longitude	Profile label	Dose rate ($\mu Sv\,h^{-1}$)	Annual dose rate ($mSv\,yr^{-1}$)
37.688264	140.995708	P1	0.2	0.8
37.721432	140.870119	P2	0.4	1.9
37.724665	140.790469	P3	1.2	6.1
37.691504	140.886210	P4	0.5	2.4
37.642013	141.015405	P5	0.1	0.3
37.654186	140.896448	P6	1.5	7.7
37.674029	140.703817	P7	2.7	14.0
37.662245	140.710906	P8	2.3	11.9
37.613850	140.800832	P9	5.5	28.7
37.621797	140.695852	P10	2.5	12.9

SOILD
1, 401–428, 2014

Depth distribution of radiocesium in Fukushima paddy fields

H. Lepage et al.

Table 2. Characteristics of the soil cores calculated for the uppermost 5 cm incremental layers. More detail could be found in the Supplement.

Core	Class	^{137}Cs inventory (%)	Bulk density (g cm^{-3})	h_0 (kg m^{-2})	α (cm^{-1})	Mean TOC (%)
P1	Managed	99.7	1.3 ± 0.3	20.4	0.87	1.0 ± 0.1
P2	Tilled	81.5	1.2 ± 0.2	n/a	n/a	1.5 ± 0.2
P3	Managed	93.3	0.8 ± 0.2	17.4	0.42	4.5 ± 0.2
P4	Tilled	84.2	0.8 ± 0.2	n/a	n/a	1.5 ± 0.1
P5	Uncontaminated	93.1	1.2 ± 0.2	n/a	n/a	n/a
P6	Undisturbed	99.4	1.2 ± 0.1	6.3	1.78	1.6 ± 0.3
P7	Undisturbed	99.7	0.9 ± 0.2	8.3	0.94	2.3 ± 0.2
P8	Managed	98.5	1.1 ± 0.2	10.4	1.05	2.1 ± 0.4
P9	Undisturbed	98.5	0.7 ± 0.1	5.4	0.93	8.5 ± 0.3
P10	Managed	97.1	0.8 ± 0.1	16.8	0.31	4.2 ± 0.4

n/a: not available

SOILD
1, 401–428, 2014

Table 3. Literature review of studies investigating evolution of radiocesium activities with depth in soils contaminated by FDNPP radioactive fallout.

Shape	Reference	Sampling period (mm/yy)	Number of samples	Type of land use investigated	Max depth (cm)	Max (kBq kg^{-1})	% upper 5 cm	α (cm^{-1})	h_0 (kg m^{-2})
Disturbed (Tilled)	Endo et al. (2013)	10/11	3	Paddy field	30	≈ 4	≈ 50	n/a	n/a
	Koarashi et al. (2012)	06/11	6	Croplands (with one paddy field)	< 20	2	81	n/a	n/a
	Matsunaga et al. (2013)	07/11	6	Croplands (with one paddy field)	< 20	1	80	n/a	n/a
	Tanaka et al. (2013)	09/12	3	Cultivated paddy field	30	7	55	n/a	n/a
	This study	11/13	2	Paddy field	10	2	83	n/a	n/a
Disturbed (managed, grazing)	Takahashi et al. (2014)	06/11	2	Land	10	33	99	0.3	n/a
			3	Field	10	39	98	1.0	n/a
		01/12	2	Land	10	130	99	0.5	n/a
			3	Field	10	40	98	0.6	n/a
		08/12	2	Land	10	130	100	0.7	n/a
			3	Field	10	28	94	0.5	n/a
		12/12	2	Land	10	110	98	0.4	n/a
			3	Field	10	38	88	0.6	n/a
	This study	11/13	4	Paddy field	10	28	97	0.7	18.2
Undisturbed	Fujiwara et al. (2012)	04/11	1	Brown forest soil	< 30	n/a	n/a	0.7	n/a
			1	Fluvisol	30	n/a	n/a	0.9	n/a
			1	Vegetable field	30	n/a	n/a	2	n/a
	Kato et al. (2011)	04/11	1	Cultivated soil (home garden)	30	9	99	1.2	9.1
	Koarashi et al. (2012)	06/11	6	Croplands (with one paddy field)	< 20	6	99	1.3	5.3
			4	Grassland	< 15	10	99	1.2	4.9
			5	Forest	< 20	3	97	0.6	8.4
	Lepage et al. (2014)	04/11	1	Cropland	2	49	n/a	1,9	7.1
	Matsunaga et al. (2013)	07/11	6	Croplands (with one paddy field)	< 20	8	99	n/a	n/a
			4	Grassland	< 20	8	99	n/a	n/a
			5	Forest	< 20	6	97	n/a	n/a
	Takahashi et al. (2014)	06/11	3	Forest	10	16	98	0.7	n/a
			2	Land	10	76	100	2.0	n/a
		01/12	3	Forest	10	100	92	0.6	n/a
			2	Land	10	440	100	1.7	n/a
		08/12	3	Forest	10	110	96	0.7	n/a
			2	Land	10	360	100	1.4	n/a
		12/12	3	Forest	10	78	94	0.7	n/a
			2	Land	10	320	100	1.3	n/a
	Tanaka et al. (2012)	04/11	2	Field	30	4	95	n/a	n/a
			2	Fruit trees field	30	3	92	n/a	n/a
	Teramage et al. (2014)	01/12	1	Coniferous forest	< 30	1	92	0.6	11.1
	This study	11/13	3	Paddy field	10	155	99	1.2	6.7

n/a: not available

SOILD

1, 401–428, 2014

Depth distribution of radiocesium in Fukushima paddy fields

H. Lepage et al.

Table 4. Estimation of the contamination in polished rice using Eq. (4). Contamination above the permissible level (100 Bq kg^{-1}) fixed by Japanese authorities is indicated in bold (MHLW, 2011).

Core	Mean activity (Bq kg^{-1}) in the first 15 cm soil layer	Estimated activity in polished rice (Bq kg^{-1})
P1	300	3
P2	1500	15
P3	1000	10
P4	2000	20
P5	20	< 1
P6	1800	18
P7	15 000	150
P8	9000	90
P9	33 000	330
P10	12 500	125

SOILD
1, 401–428, 2014

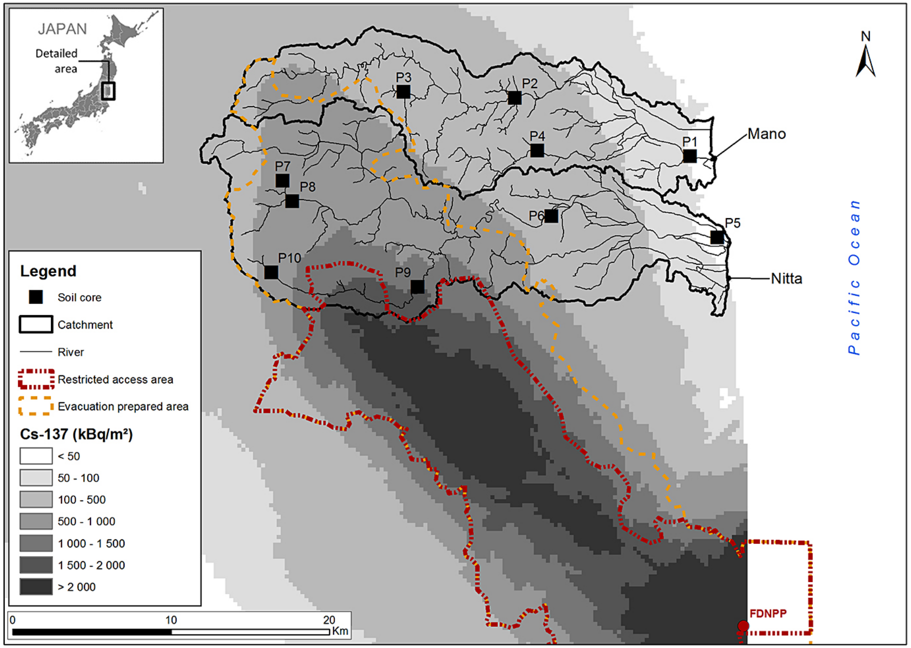

Figure 1. Map of the study area with location of the soil cores collected within Mano and Nitta River catchments. The map represents ^{137}Cs soil inventory decay corrected to the date of 14 June 2011 based on the Japanese Ministry of Education, Culture, Sports, Science and Technology data (MEXT, 2012) with April 2014 restricted access areas delineated (METI, 2014).

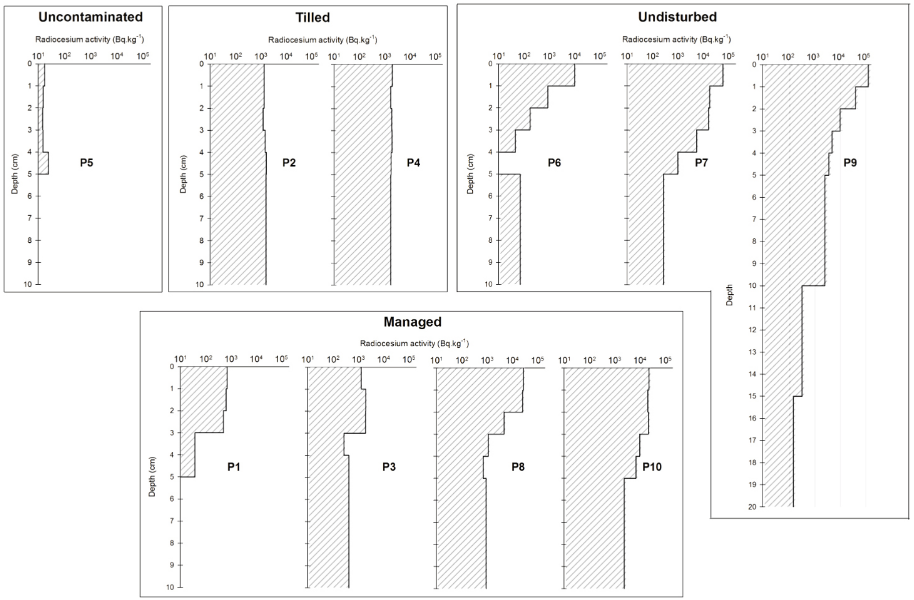

Figure 2. Depth migration in soil cores. Data on 4–5 cm layer for P6 were not available.

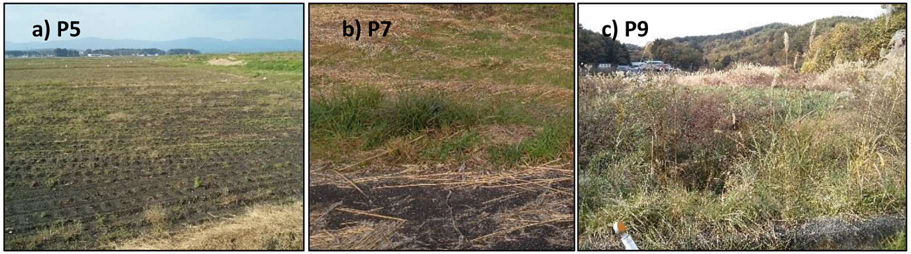

Figure 3. Pictures taken during the sampling campaign (November 2013) and illustrating the difference of land management practices in the field **(a)** P5 – land management in the field showed by tractor tracks **(b)** P7 – grass recently cut and presence of straw residues on the field **(c)** P9 – dense cover of grass on the field show an absence of land management.

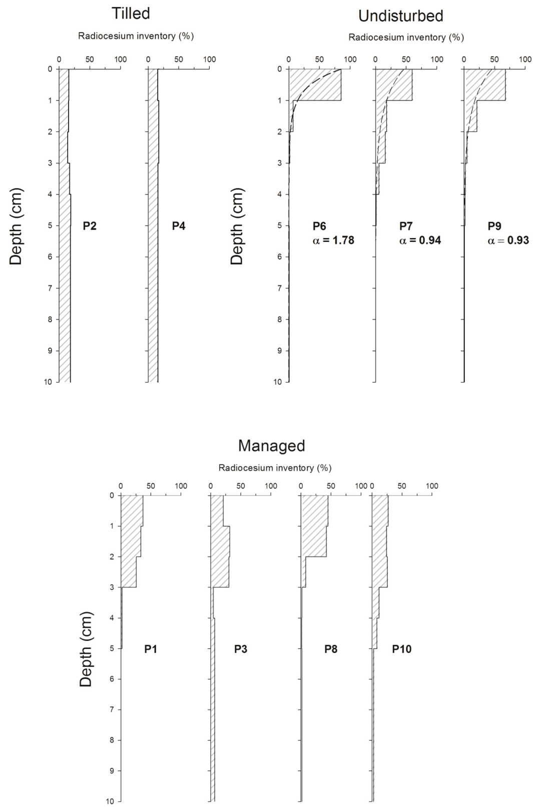

Figure 4. Depth migration of radiocesium in the different groups of contaminated soil cores.

SOILD
1, 401–428, 2014

Depth distribution of radiocesium in Fukushima paddy fields

H. Lepage et al.

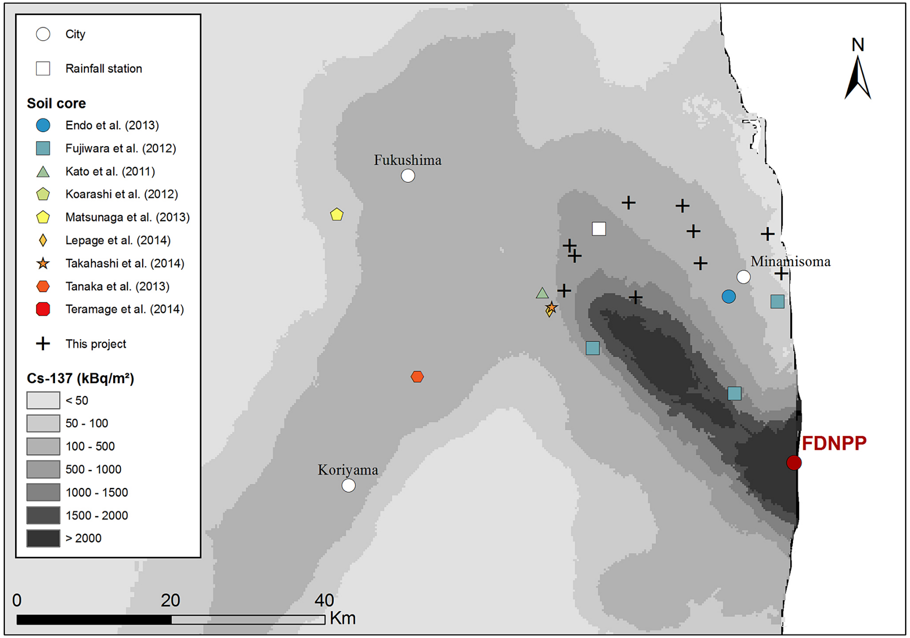

Figure 5. Location of soil cores analysed in previous studies and map of the main radiocesium plume in Fukushima Prefecture. Soil sample investigated by Teramage et al. (2014) was collected at approximately 100 km to the south of Koriyama. Koarashi et al. (2012) and Matsunaga et al. (2013) sampled at the same location.

SOILD
1, 401–428, 2014

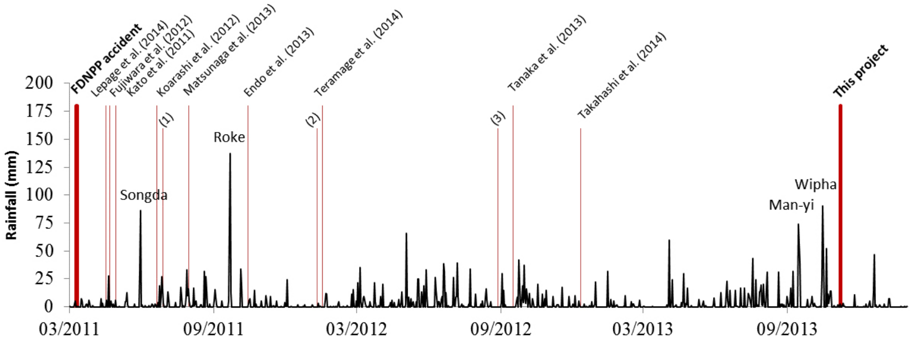

Figure 6. Cumulative rainfall between FDNPP accident and this sampling campaign. Occurrence of typhoons is indicated on the graph. Timing of sampling campaigns of previous studies dealing with radiocesium migration in soils is also indicated. Takahashi et al. (2014) also sampled at (1) (2) and (3).

SOILD
1, 401–428, 2014

Depth distribution of radiocesium in Fukushima paddy fields

H. Lepage et al.